Cell Reports, Volume *24*

Supplemental Information

BET Inhibition-Induced GSK3β Feedback Enhances Lymphoma Vulnerability to PI3K Inhibitors

Enrico Derenzini, Patrizia Mondello, Tatiana Erazo, Ana Portelinha, Yuxuan Liu, Mary Scallion, Zahra Asgari, John Philip, Patrick Hilden, Debora Valli, Alessandra Rossi, Hakim Djaballah, Ouathek Ouerfelli, Elisa de Stanchina, Venkatraman E. Seshan, Ronald C. Hendrickson, and Anas Younes

Supplementary information

Supplemental figures and legends

Fig. S1

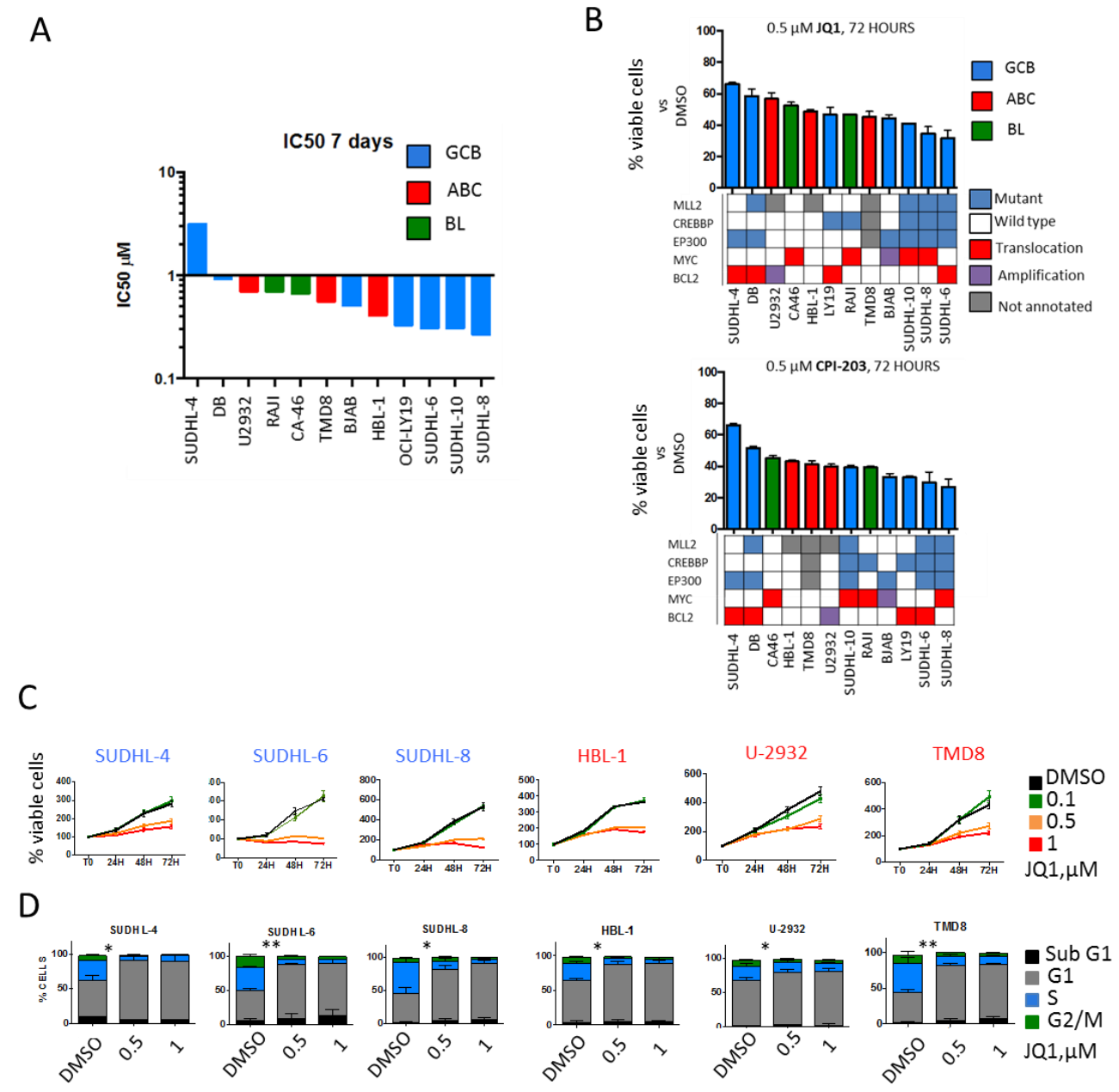
A
IC50 7 days
GCB
ABC
BL
IC50 µM
SUDHL-4
DB
U2932
RAJI
CA-46
TMD8
BJAB
HBL-1
OCI-LY19
SUDHL-6
SUDHL-10
SUDHL-8
B
0.5 µM JQ1, 72 HOURS
% viable cells vs DMSO
MLL2
CREBBP
EP300
MYC
BCL2
Mutant
Wild type
Translocation
Amplification
Not annotated
0.5 µM CPI-203, 72 HOURS
C
SUDHL-4
SUDHL-6
SUDHL-8
HBL-1
U-2932
TMD8
% viable cells
T0
24H
48H
72H
DMSO
0.1
0.5
1
JQ1,µM
D
% CELLS
Sub G1
G1
S
G2/M
JQ1,µM

Figure S1. Antiproliferative activity of JQ1 in aggressive B-cell lymphoma cell lines. Related to figure 1.

A) Bar graph showing 7 day-IC 50 values of our B-cell lymphoma cell line panel (n=12), treated with the bromodomain inhibitor JQ1, in a logarithmic scale. Results are from an automated drug screening assay.

B) Bar graphs showing the efficacy of treatment with JQ1 and CPI-203 0.5 μM for 72 hours in our cell line panel, with respect to the cell of origin and the presence of absence of recurrent mutations of histone modifiers genes, MYC and BCL-2 rearrangements. Viability was determined by MTS assay. Mutations were annotated according to Cancer Cell Line Encyclopedia (http://www.broadinstitute.org/ccle/home), and Pasqualucci et al, 2011; and Zhang et al, 2013. Error bars represent standard error of the mean (S.E.M) of triplicate experiments.

C) MTS assay of 6 representative DLBCL cell lines treated with 0.1, 0.5 and 1 μM JQ1 for 24, 48, 72 hours. Cell viability is plotted vs T0. Error bars represent S.E.M of triplicate experiments.

D) Cell cycle analysis of 6 representative DLBCL cell lines treated with 0.5 and 1 μM JQ1 for 72 hours, showing significant increase in the G1 cell cycle fraction after treatment with JQ1. Error bars represent S.E.M of triplicate experiments. P values were calculated with the Student`s T test * $p< 0.05$, ** $p<0.01$.

Fig. S2

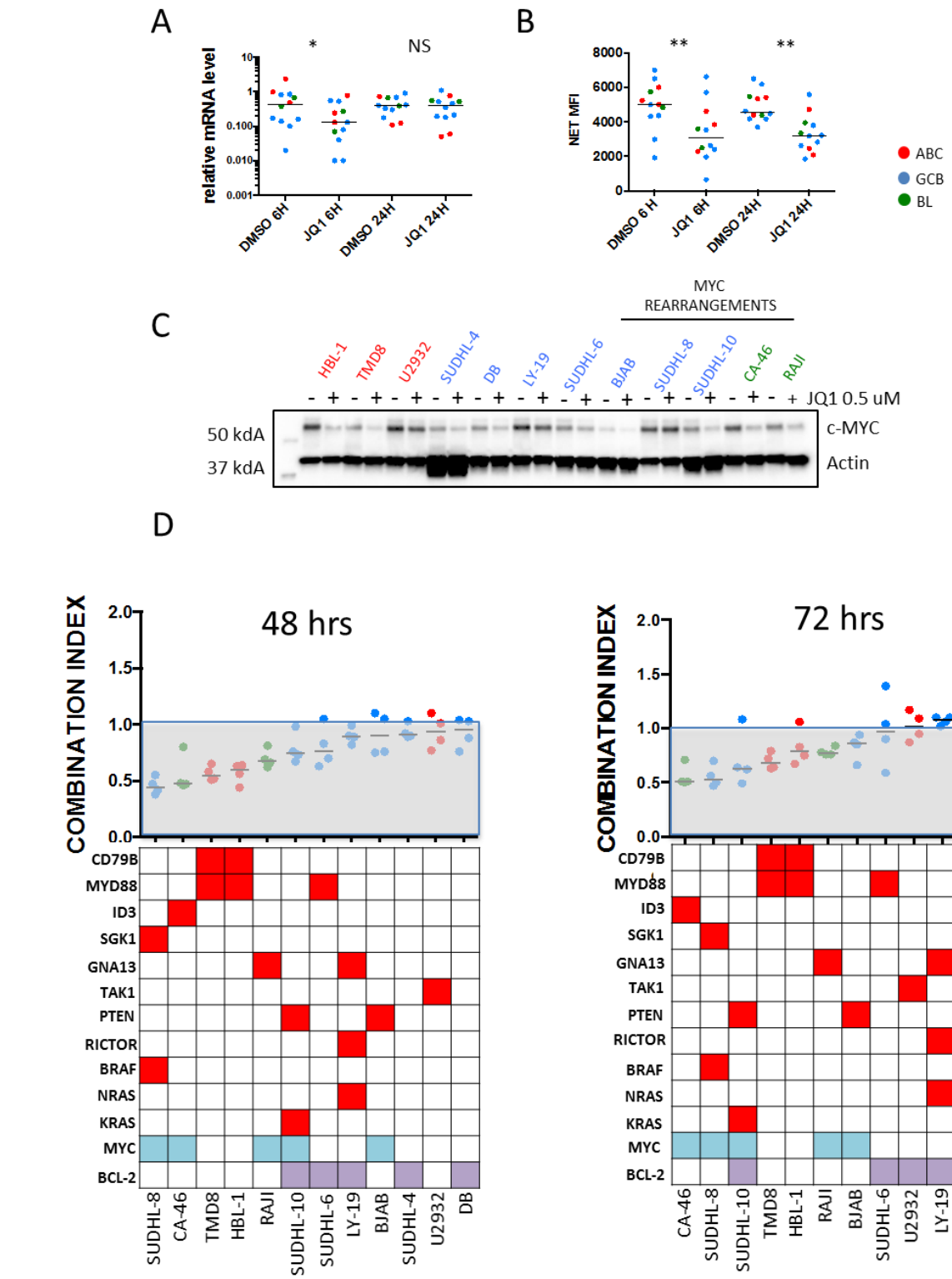
A
relative mRNA level
*
NS
DMSO 6H
JQ1 6H
DMSO 24H
JQ1 24H
B
NET MFI
**
**
ABC
GCB
BL
C
MYC REARRANGEMENTS
HBL-1
TMD8
U2932
SUDHL-4
DB
LY-19
SUDHL-6
BJAB
SUDHL-8
SUDHL-10
CA-46
RAJI
JQ1 0.5 uM
50 kdA
37 kdA
c-MYC
Actin
D
48 hrs
72 hrs
COMBINATION INDEX
CD79B
MYD88
ID3
SGK1
GNA13
TAK1
PTEN
RICTOR
BRAF
NRAS
KRAS
MYC
BCL-2
SUDHL-8
CA-46
TMD8
HBL-1
RAJI
SUDHL-10
SUDHL-6
LY-19
BJAB
SUDHL-4
U2932
DB

Figure S2. JQ1 downregulates MYC and enhances the antiproliferative activity of the PI3K inhibitor BKM-120 in DLBCL and BL cell lines. Related to figure 1.

A) Scatterplot showing the effects of JQ1 on relative *MYC* mRNA levels in our cell line panel. Cells where incubated with JQ1 0.5 μM for 6 and 24 hours and MYC expression levels were assessed by qPCR. P values were calculated with the Wilcoxon Rank test. * $p< 0.05$, ** $p<0.01$.

B) Scatterplot showing the effects of JQ1 on c-MYC protein levels in our cell line panel. Cells where incubated with DMSO or JQ1 0.5 μM for 6 and 24 hours and c-MYC expression levels were assessed by luminex. Mean c-MYC fluorescence intensity levels were normalized to beta tubulin levels. Median c-MYC downregulation at 24 hours across all cell lines was 0.65 (35%). P values were calculated with the Wilcoxon Rank test. * $p< 0.05$, ** $p<0.01$.

C) Representative western blot assay confirming decreased c-MYC expression levels after 6 hours incubation with JQ1 0.5 μM.

D) Scatterplots summarizing the results of our MTS assay validation of the HT screening data at 48 and 72 hrs. Cells were incubated with increasing concentrations (0.25, 0.5, 0.75 and 1μM) of JQ1 and BKM-120, and the combination index was calculated according to the Chou-Talalay method from the average of 3 independent experiments. Genomic alterations of MYC, BCL-2 and genes involved in PI3K and BCR signaling are represented in the heat map. Mutations were annotated according to Cancer Cell Line Encyclopedia (http://www.broadinstitute.org/ccle/home), and Davis et al 2010, Ngo et al, 2011, Fontan et al, 2012

Fig. S3

	CA-46	HBL-1	TMD8	U2932	DB	LY-19	SUDHL-4	SUDHL-6	SUDHL-8
AKT1	4.0	1.1	1.0	1.1	1.4	1.1	1.3	1.3	0.8
AKT2	3.9	1.0	0.8	1.1	1.1	0.7	1.2	1.0	1.1
BAD	2.8	1.0	1.0	0.9	1.0	0.5	1.4	0.8	0.5
BCL2	BD	1.7	2.2	0.9	0.8	1.7	0.4	0.4	0.4
BCL2L1	2.5	1.0	3.2	0.5	0.9	0.8	1.0	0.6	0.7
CASP9	5.5	1.5	1.5	1.3	1.6	1.6	1.6	1.4	1.3
CCND1	BD	0.6	0.5	0.3	BD	BD	BD	BD	BD
CCND2	BD	0.6	1.1	0.4	0.6	0.3	0.3	0.8	0.8
CCND3	0.5	1.0	0.6	1.0	0.9	0.4	0.8	0.6	0.3
CDH1	0.8	BD	2.9	BD	BD	BD	BD	BD	BD
CDKN1A	0.4	1.2	1.1	1.4	2.5	1.6	1.5	1.4	2.1
CHUK	1.3	1.1	1.2	1.1	1.0	1.2	1.1	1.2	1.1
COL1A1	0.3	15.1	1.4	0.8	0.9	0.5	0.6	3.8	1.5
CREB1	1.7	1.2	1.5	1.2	1.6	1.3	1.5	1.3	1.3
CRP	BD	4.9	2.8	BD	0.7	BD	5.3	5.4	3.1
CTNNB1	1.8	1.3	1.5	1.3	1.7	1.3	1.5	1.4	1.4
EIF4EBP1	0.8	0.6	0.5	0.9	0.6	0.7	0.8	0.5	0.8
ELK1	1.1	1.2	1.0	1.1	1.0	1.0	1.0	1.0	0.9
ERBB2	2.0	1.6	1.2	1.3	1.5	1.0	1.1	2.2	1.3
FOS	6.1	2.1	20.9	3.1	1.6	1.8	1.9	5.7	3.4
FOXO3	1.2	1.8	1.5	1.0	1.1	1.5	2.0	1.2	1.6
GRB2	1.6	1.2	1.3	1.2	1.1	1.0	1.1	0.9	1.1
GSK3A	1.3	1.0	1.1	1.0	1.1	0.3	1.1	1.0	0.9
GSK3B	2.2	1.5	2.1	1.6	1.8	2.1	1.9	1.7	2.2
GYS1	1.4	1.4	1.5	1.1	1.2	1.2	1.6	1.5	1.2
HIF1A	1.6	1.0	1.5	1.0	1.5	1.3	1.9	1.6	1.2
HRAS	1.0	0.9	0.9	0.9	0.8	0.7	0.9	0.8	0.6
IGF1	BD	BD	BD	0.2	BD	BD	BD	BD	BD
IGF1R	1.6	1.6	1.7	1.3	0.4	1.6	0.6	1.5	1.2
IGF2	2.5	0.6	4.2	BD	1.1	2.6	5.2	4.5	2.0
IGFBP2	0.1	1.0	0.1	1.0	0.1	0.0	BD	BD	0.1
IGFBP3	BD	BD	BD	2.0	BD	BD	BD	BD	BD
IGFBP4	BD	3.0	1.1	0.6	0.8	0.4	1.5	2.4	0.7
IGFBP5	BD	BD	3.1	BD	0.6	0.0	1.5	5.6	1.0
IGFBP6	0.3	2.8	0.1	0.8	0.4	1.0	0.3	0.2	2.3
IKBKB	1.4	1.0	1.4	0.9	1.1	1.2	1.1	1.4	1.1
IL6	BD	0.4	0.4	BD	BD	BD	BD	BD	BD
IRS1	1.2	0.7	0.5	0.9	0.5	0.7	0.7	0.9	0.6
IRS2	1.3	2.0	1.0	1.3	BD	1.2	0.7	BD	BD
JUN	2.8	1.2	1.3	1.8	1.6	1.5	1.8	3.3	2.9
MAP2K1	1.3	1.5	1.4	1.3	1.3	1.4	1.5	1.3	1.5
MAP2K2	1.6	1.2	1.3	1.2	1.2	1.5	1.3	1.0	1.5
MAP3K5	1.0	0.6	0.7	1.0		1.1	0.9	1.0	1.0
MAPK1	1.6	1.2	1.3	1.1	1.5	1.1	1.4	1.4	1.1
MAPK3	0.4	0.5	0.3	0.5	0.6	0.2	0.5	0.3	0.1
MTOR	1.6	1.2	1.3	1.3	1.7	1.6	1.0	1.2	1.3
MYC	1.0	0.6	0.5	1.1	0.8	0.9	0.6	1.0	1.3
NFKB1	1.5	1.2	3.5	0.8	1.0	0.9	1.2	0.9	1.1
NFKB2	1.5	0.8	2.5	0.6	0.9	1.0	1.2	1.2	1.2
NFKBIA	2.1	1.1	4.8	1.0	2.8	1.1	2.8	1.1	0.9
NFKBIB	0.7	0.6	1.8	0.6	0.6	0.6	0.8	0.6	0.8
NFKBIE	1.2	1.4	2.0	0.5	1.2	1.0	0.9	1.0	0.9
PDPK1	1.8	1.7	1.4	1.5	2.3	1.9	1.3	1.9	1.8
PIK3CA	2.5	1.5	2.1	1.2	1.4	1.5	1.3	2.8	1.8
PIK3CB	1.5	1.4	1.8	1.3	1.2	1.3	1.1	1.3	1.0
PIK3CD	0.9	0.9	1.1	0.6	1.7	0.9	0.8	0.9	0.7
PIK3R1	1.5	1.6	2.1	1.6	1.9	1.3	1.9	1.7	1.4
PIK3R2	1.7	1.1	1.0	1.1	1.4	1.1	1.0	1.0	1.2
PIK3R3	1.1	0.9	1.1	1.1	0.8	1.1	2.7	1.2	0.7
PTEN	1.4	1.2	1.0	0.8	2.2	1.0	1.0	0.7	0.9
PTGS2	BD	1.0	BD	BD	BD	BD	BD	BD	BD
RAF1	1.4	1.1	1.1	1.0	1.2	1.0	1.0	1.1	1.1
REL	2.0	1.8	4.2	1.2	1.1	1.5	1.5	1.5	1.5
RELA	1.3	1.1	1.2	1.2	1.4	1.3	1.3	1.2	1.2
RELB	1.6	1.0	2.4	0.7	1.0	1.1	1.8	1.3	1.0
RHEB	1.2	1.1	1.3	1.0	1.2	1.0	1.0	1.2	0.8
RPS6KA1	1.1	1.0	1.1	0.8	1.1	1.0	1.0	0.9	0.7
RPS6KA2	3.3	2.3	2.2	1.3	0.9	1.7	2.4	0.8	0.8
RPS6KA3	1.4	1.0	1.8	0.9	1.3	1.2	1.0	1.1	0.9
RPS6KB1	1.8	1.1	1.3	1.3	1.3	1.4	1.2	1.5	1.3
SERPINE1	3.1	0.8	BD	1.9	8.1	BD	1.6	2.6	0.9
SHC1	1.1	1.1	0.8	0.8	0.8	1.2	1.2	1.0	1.1
SOS2	2.1	1.9	1.9	1.5	1.5	1.7	1.8	1.9	1.6
SP1	1.0	1.0	0.8	0.9	0.9	0.9	0.7	0.8	0.6
SPP1	1.3	0.6	0.8	19.7	BD	0.2	0.6	BD	1.1
STAT3	2.8	0.7	0.8	1.8	3.0	1.8	1.7	2.3	2.0
TGFB1	1.7	1.4	1.2	1.4	1.4	1.4	1.0	1.4	1.8
TSC1	1.7	1.5	1.7	1.2	2.1	1.4	1.1	1.7	1.4
TSC2	1.9	1.4	1.6	1.5	1.5	1.1	1.8	1.5	1.3
UBA52	0.5	0.8	0.6	0.6	0.5	0.6	0.5	0.4	0.6
UBB	1.6	1.1	1.3	1.2	1.4	1.3	1.5	1.4	1.1
UBC	1.1	1.3	1.4	1.1	1.1	1.4	1.0	1.0	1.3
VEGFA	0.5	0.7	1.3	0.8	0.8	0.7	1.1	0.9	0.9
YWHAB	1.6	1.2	1.3	1.1	1.3	1.0	1.0	1.2	1.1
YWHAE	1.4	1.0	1.1	1.1	1.1	1.1	0.9	1.1	0.9
YWHAZ	1.6	1.3	1.3	1.0	1.2	1.4	1.4	1.3	1.1

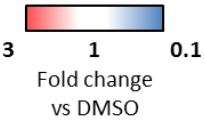

Figure S3. Effect of JQ1 on PI3K pathway gene expression in DLBCL and BL cell lines. Related to figure 2.

Heat map showing fold change values of PI3K pathway components in DLBCL and BL cells after incubation with JQ1 0.5μM for 24 hours. Fold change values of JQ1-treated cells vs DMSO are represented in a colorimetric scale from blue (low) to red (high).

Fig. S4

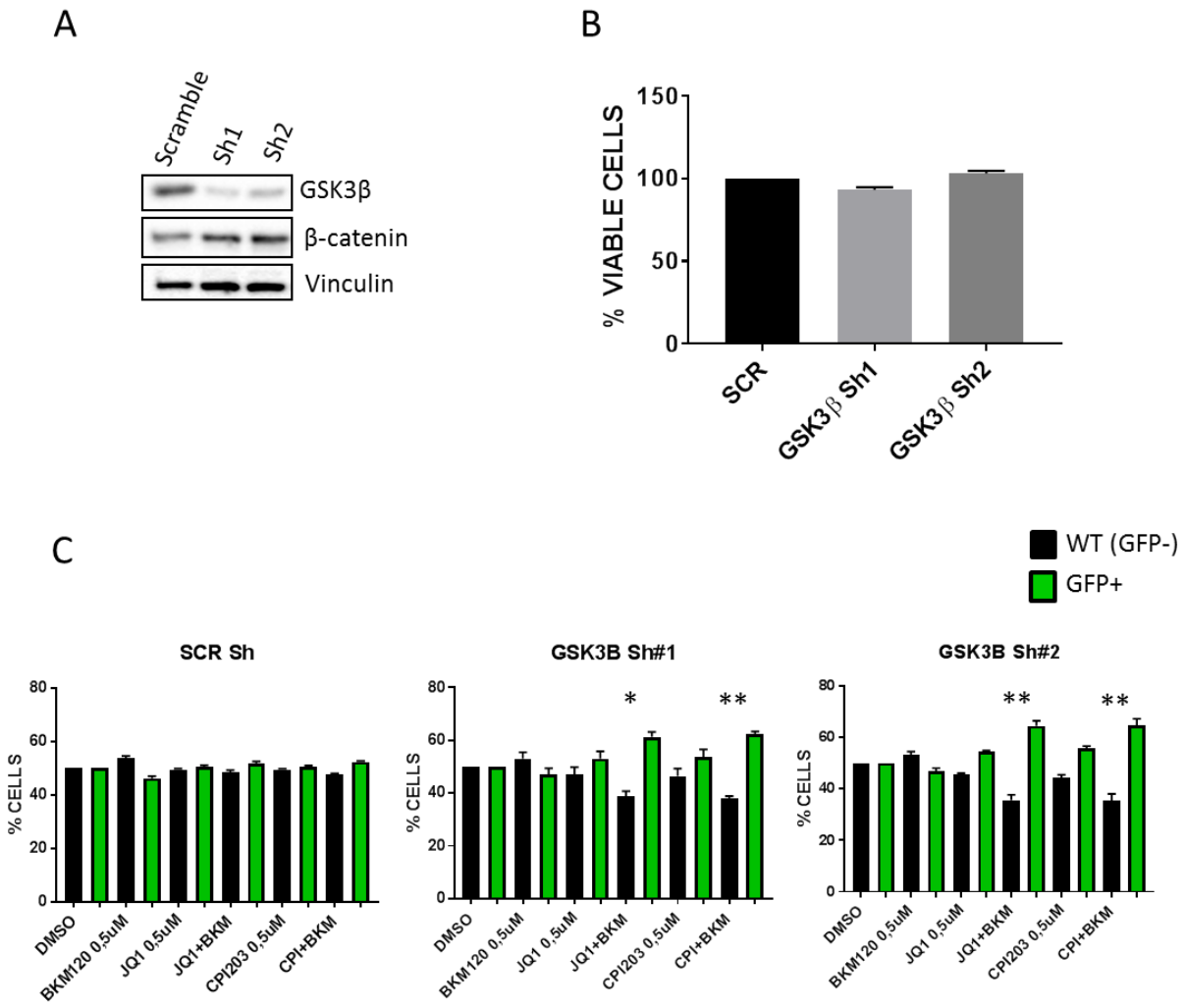

Figure S4. Effects of GSK3β depletion in TMD8 cells. Related to figure 4.

A) Western blot confirming effective *GSK3β* silencing and β-catenin induction after 72 hours of doxycycline (1µg/ml) treatment in TMD8 cells with 2 different *GSK3β* ShRNAs (GSK3β.1, GSK3β.2) vs scramble (SCR).

B) MTS assay showing lack of effect of *GSK3β* silencing on cell proliferation after 72 hours of doxycycline induction in TMD8 cells. Error bars represent S.E.M of triplicate experiments.

A) Bar graphs showing full data of the competitive proliferation assay experiment showed in figure 4F. Briefly, mixtures of GFP positive (scramble, Sh#1 and Sh#2 transduced TMD8 cells) and GFP negative (wild type) cells were induced with 1 µg/ml doxycycline for 72 hours and then incubated with the indicated compounds for additional 72 hours. Then, the % of GFP positive cells in each condition was assessed by flow cytometry. Error bars represent S.E.M of triplicate experiments. Differences between groups (WT vs GFP+ cells) were calculated with the Student T test. * $p< 0.05$, ** $p<0.01$.

Fig. S5


A
MYC-OFF
#1
#2
EXP
MYC
EIF4EBP1
UBA52
PIK3R2
IGF1
MAPK3
GSK3A
MAP2K2
HIF1A
MAPK1
TSC1
UBB
YWHAB
GRB2
RPS6KA3
BAD
PTEN
SHC1
AKT2
SP1
RELA
CCND2
GYS1
UBC
GSK3B
RPS6KA1
REL
CTNNB1
CCND3
NFKB1
PIK3CA
RPS6KA2
CASP9
YWHAZ
CCND1
CREB1
PIK3R1
IKBKB
STAT3
SOS2
RELB
BCL2
PIK3CD
ERBB2
NFKBIE
NFKB2
COL1A1
NFKBIA
CDH1
BCL2L1
IL6
JUN
IGFBP4
5
1
0.1
Fold change
vs DMSO
B
MYC-OFF
30 Min
24 hrs
p-PTEN
p-Akt
p-GSK3-beta
p-GSK3-alpha
p-TSC2
p-mTOR
p-p70S6K
2
1
0.1
Fold change
vs DMSO

Figure S5. MYC dependent regulation of PI3K pathway gene expression and activation in P-4936 cells. Related to figure 5.

A) Heat map showing fold change values of significantly deregulated (>±1.5 average fold change) PI3K pathway-related genes in P-4936 cells after MYC depletion (MYC-OFF), for 24 hours.

B) Effects of MYC silencing for 24 hours (MYC-OFF), on phosphorylation levels of PI3K pathway components, as determined by a PI3K pathway dedicated luminex multiplex assay in P-4936 cells. Average fold change values obtained in 3 independent experiments are represented in a colorimetric scale from blue (low) to red (high).

Fig. S6

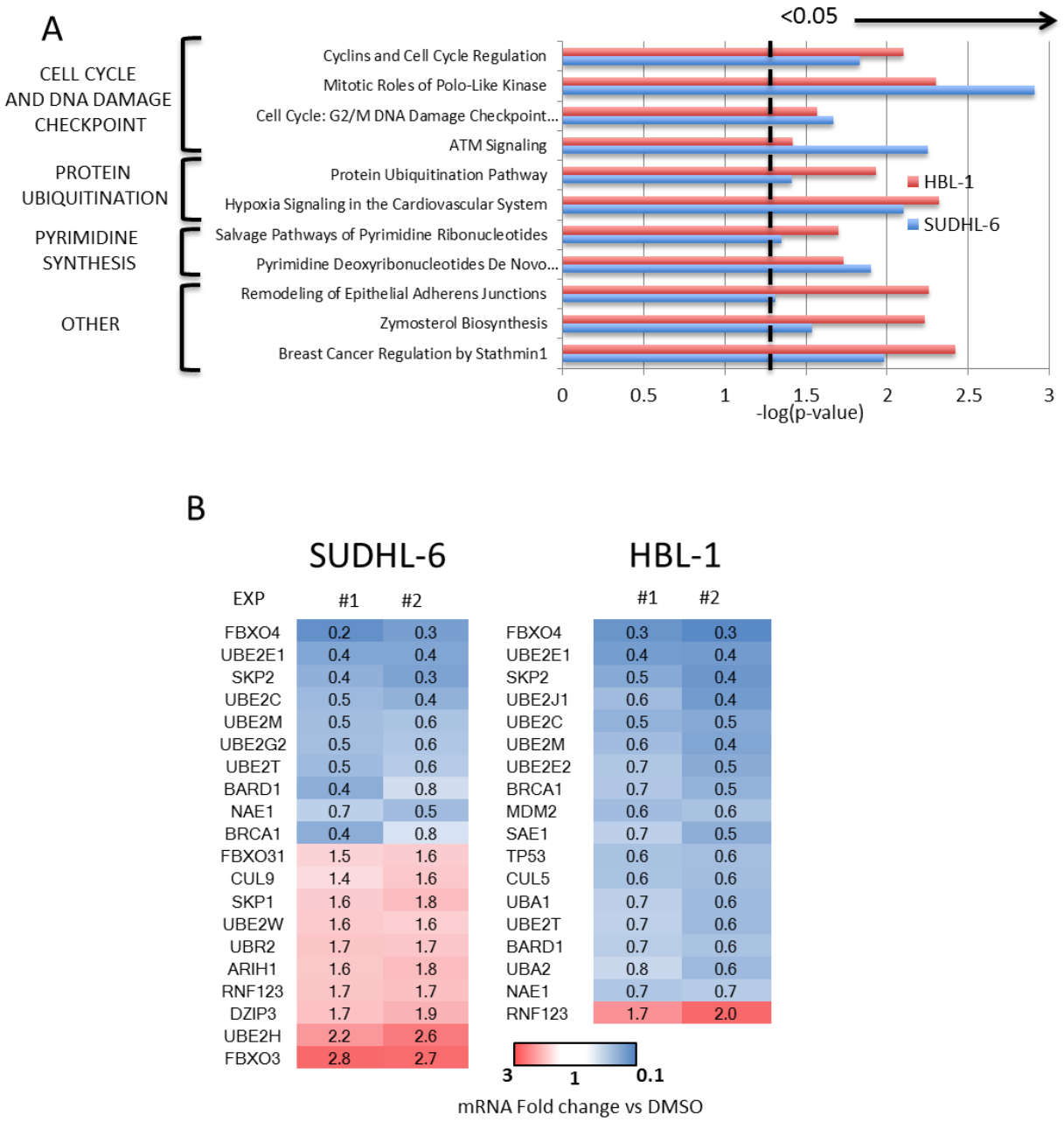

Figure S6. JQ1 deregulates ubiquitination pathway components in DLBCL. Related to figure 6.

A) Ingenuity pathway analysis of SILAC mass spectrometry data showing top 11 commonly regulated pathways in HBL-1 and SUDHL-6 cells after treatment with JQ1 0.5 μM for 24 hours (p-value was calculate with right tailed Fisher`s exact test).

B) Effects of JQ1 on significantly down and upregulated genes (average fold change > +/- 1.5) belonging to protein ubiquitination pathways in SUDHL-6 and HBL-1 cells. Fold change values vs DMSO obtained in 2 independent experiments are depicted in the heat map with a colorimetric scale.

Fig. S7

A

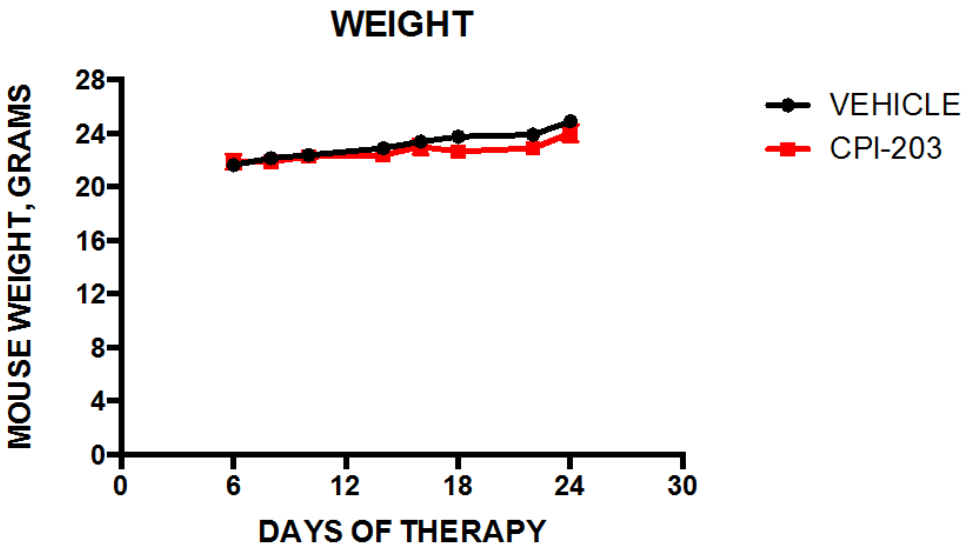
WEIGHT
MOUSE WEIGHT, GRAMS
28
24
20
16
12
8
4
0
0
6
12
18
24
30
DAYS OF THERAPY
VEHICLE
CPI-203

B

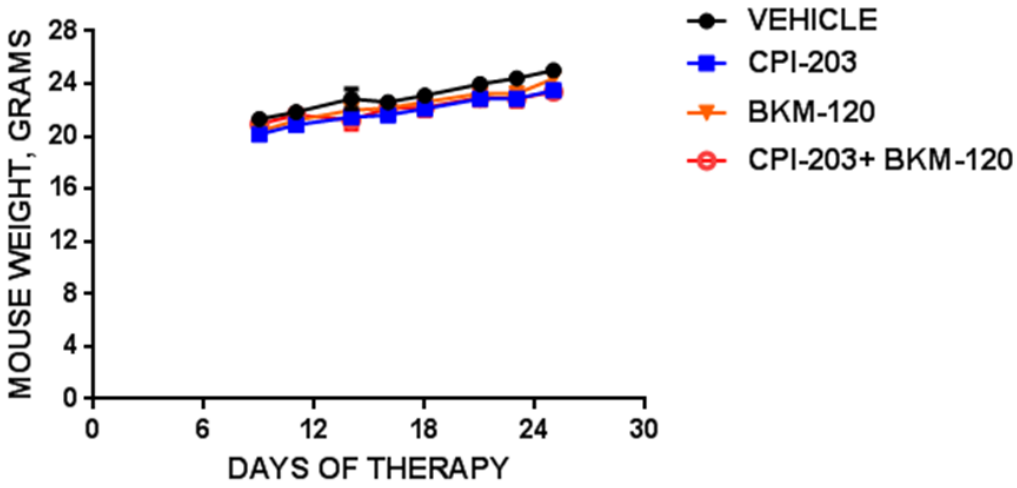
MOUSE WEIGHT, GRAMS
28
24
20
16
12
8
4
0
0
6
12
18
24
30
DAYS OF THERAPY
VEHICLE
CPI-203
BKM-120
CPI-203+ BKM-120

Figure S7. Toxicity of in vivo single agent BET inhibition or combined BET and PI3K inhibition in DLBCL mouse xenografts. Related to figure 7.

A) Graph showing variations of body weight over time in TMD8 xenografts treated with CPI-203 5 mg/kg twice daily.

B) Graph showing variations of body weight over time in TMD8 xenografts treated with vehicle (n=8) CPI-203 5 mg/kg twice daily (n=8), BKM-120 15 mg/Kg daily (n=8), and the combination (n=8).

References (supplementary figures)

Davis RE, Ngo VN, Lenz G, Tolar P, Young RM, Romesser PB, Kohlhammer H, Lamy L, Zhao H, Yang Y, et al. (2010). Chronic active B-cell-receptor signalling in diffuse large B-cell lymphoma. Nature *463*, 88-92.

Fontan L, Yang C, Kabaleeswaran V, Volpon L, Osborne MJ, Beltran E, Garcia M, Cerchietti L, Shaknovich R, Yang SN, Fang F, et al. (2012). MALT1 small molecule inhibitors specifically suppress ABC-DLBCL in vitro and in vivo. Cancer Cell *22*, 812-24.

Ngo VN, Young RM, Schmitz R, Jhavar S, Xiao W, Lim KH, Kohlhammer H, Xu W, Yang Y, Zhao H et al. (2011). Oncogenically active MYD88 mutations in human lymphoma. Nature *470*, 115-9.

Pasqualucci L, Dominguez-Sola D, Chiarenza A, Fabbri G, Grunn A, Trifonov V, Kasper LH, Lerach S, Tang H, Ma J et al. (2011). Inactivating mutations of acetyltransferase genes in B-cell lymphoma. Nature *471*, 189-95.

Zhang J, Grubor V, Love CL, Banerjee A, Richards KL, Mieczkowski PA, Dunphy C, Choi W, Au WY, Srivastava G et al. (2013). Genetic heterogeneity of diffuse large B-cell lymphoma. Proc Natl Acad Sci USA *110*, 1398-403.

Supplemental methods

High-Throughput Drug Screening

Single Agent Dose Response Studies. For the single agent studies, 1 µL of compounds were pre-plated in a 12 point doubling dilution series with 100 µM compound concentration as the upper limit and transferred from an intermediate 384-well polypropylene microtiter plate (Thermo Scientific, Waltham, MA) to a 1536-well microtiter assay plate (Corning, Corning, NY) using the custom-designed 384 head on a PP-384-M Personal Pipettor (Apricot Designs, Monrovia, CA).

For internal reference, each assay plate contained at a final concentration 1% DMSO (v/v) vehicle only as the high control in Row A-B and a 1 uM of killer mix in 1% DMSO (v/v) as the low control in Row EE-FF. To start the assay, cells were seeded at 1,000 cells per well in 8 µL of complete RPMI medium using the FlexDrop IV (Perkin Elmer, Waltham, MA) and incubated for 6 days at 37°C for compound treatment. Next, 1 µL AB was added and further incubated for an additional day at 37°C followed by imaging on the LEADseeker™ Multimodality Imaging System (GE Healthcare, Piscataway, NJ) for resulting fluorescence intensity. Dose response curves for each data set was fitted separately and the two obtained IC_{50} values were averaged for reporting.

***HTS statistical analysis*.** The drugs were tested for activity both as single agents and in combinations on multiple cell lines through the high throughput screening core facility (HTSCF). The residual cell viability post treatment with specific drug combinations was assessed in an Alamar Blue (AB) assay and quantified as fluorescence signal intensity measured using the LEADseeker Multimodality Imaging System (GE Healthcare, Piscataway, NJ). The data was converted into percent inhibitions conferred by each combination relative to both the high (1% DMSO v/v) and the low (1 µM killer mix) control averages (µ). Of note, "killer mix" consists of a HTSCF proprietary mixture of cytotoxic compounds. The percent inhibitions were defined as:

$$\%inhib_i = (\mu_{high\ control} - value_i)/(\mu_{high\ control} - \mu_{low\ control}) \times 100$$

Since the percent inhibition is derived from data measured with error some of the computed numbers can fall outside the [0, 100]% interval. We replaced such valued by the appropriate boundary value. We used the average percent inhibition of the replicates at a dose level (single agent or combination) as the activity at that dose level.

In order to evaluate whether a drug combination shows synergy we compared the observed activity at the combination at that level to the expected activity under Bliss independence model. By treating percent inhibition as a probability and using the product rule for the probability of independent events, the expected activity can be written as

$$P(Inh|A,B) = 1 - P\left(\overline{Inh}\middle|A,B\right) = 1 - P\left(\overline{Inh}\middle|A\right) \times P\left(\overline{Inh}\middle|B\right) = 1 - [1 - P(Inh|A)] \times [1 - P(Inh|B)]$$

where A and B are the two drugs, Inh and $\overline{Inh}$ denote inhibited and not inhibited respectively (Feller, 1971;Tallarida, 2001). The observed can be compared to the expected activity using a simple difference where values around 0 represent additive relationship, large positive values represent synergy and large negative values antagonism. However the same magnitude of the difference represents different relative change depending on the expected activity. Thus we also use a log-odds measure given as $\log\{[P_o(1-P_e)]/[P_e(1-P_o)]\}$ where P_o and P_e are observed and expected activities. For each drug combination we generated a heatmap for the observed inhibition, the difference between observed and expected inhibition and the log-odds of the observed to expected inhibition. The observed and expected inhibition values were rescaled prior to calculating the log-odds by the function (0.8 * observed/expected + 0.1), this was done in order to adjust for instances in which the observed or expected inhibition was 0 or 1. These numbers are binned into intervals suitable for each scale and color coded for simple visualization of the combined activity. For comparing drug combinations we combined the log-odds data across all cell lines and used the medians to rank the combinations. The data are shown as boxplots. All analyses were done using R programming language (R Core Team, 2014).

PCR pathway arrays and qPCR

Total RNA was extracted with the Qiagen (Valencia, CA) RNeasy mini kit protocol. A total of 1 ug of RNA was converted to cDNA using iScript cDNA synthesis kit (Bio-Rad). Real-time polymerase chain reaction (PCR) was performed using the model CFX96 (Biorad). The assay used were the IGF-1 receptor signaling pathway H96 (Biorad), and the human protein ubiquitination H96 panel (Qiagen, PAHS-079Z) according to manufacturer`s instructions. Gene lists for these assays can be found below. For the ubiquitination pathway array reverse transcription was performed using the RT2 first strand cDNA synthesis kit (Qiagen, cat n°330404). Primers for GAPDH, MYC, were purchased from Biorad. GAPDH (qHsaCED0038674), MYC (qHsaCID0012921).

SiRNA experiments

siRNA transfections were performed by using the Amaxa 4D –Nucleofector Unit (Lonza). MYC siRNA: Briefly, $3x10^6$ cells per condition were transfected with 1 μM siRNA or scramble, and resuspended in RPMI 10% FBS with no antibiotics. siRNAs were purchased from Life Technologies (NY, USA): MYC (#4392420: s9129, s9130), Negative Control 1 (#4390643). UBE2C and UBE2T siRNAs: A heterogeneous mixture of small interfering RNAs (siRNAs) that target human UBE2C and UBE2T mRNA sequence were purchased from Dharmacon (Smartpool ON-TARGETplus; L-004693-00-0005 and L-004898-00-005, respectively). Cells were transfected with 25nM and 75nM (per well of a six-well plate) of UBE2C and UBE2T siRNAs or control (scrambled) siRNA. Optimization was done using the Amaxa Cell Line Optimization 4D-Nucleofector X kit (#V4XC-9064). Transfection was performed using the 4D- Nucleofector X kit L (#V4XC-2024).

GSK3β ShRNA experiment

The short hairpin RNA (shRNA) was cloned into the pRSIT17-U6Tet-sh-CMV-TetRep-2A-TagGFP2-2A-Puro Vector (Cellecta), to generate stable lentiviral infected cell lines harbouring a Tet-On inducible Knock Down system.

This vector includes an inducible version of U6 shRNA promoter for Tet regulated shRNA expression, a TagGFP2 mark and a puromycin resistance gene. The shRNA were designed against the coding sequence of *GSK3β*. Sequences are the followings:

SCRAMBLE :
- shRNA for use as a negative control.
Sequence: CCTAAGGTTAAGTCGCCCTCGCTCGAGCGAGGGCGACTTAACCTTAGG

GSK3β Sh#1
Sequence: CCGGCCACAGAACCTCTTGTTGGATCTCGAGATCCAACAAGAGGTTCTGTGGTTTTTG

GSK3β Sh#2
Sequence: CCGGCATGAAAGTTAGCAGAGATAACTCGAGTTATCTCTGCTAACTTTCATGTTTTTG

Western blotting

Preparation of cellular protein lysates was performed by using the Cell Signalling lysis buffer (#9803) according to manufacturer`s extraction protocol. Protein quantitation was done using the Direct Detect system (Millipore).

A total of 30 ug of protein was denatured in Laemli buffer at 95C for 5 minutes and western immunoblotting was performed using the Biorad system (TGX 4-15% gels). Transfer was performed using the Trans Blot turbo system (Biorad) onto PVDF membranes. Images were acquired by using the BioRad Imaging Chemidoc MP system. Secondary anti-rabbit and anti-mouse HRP-conjugated antibodies were purchased from Biorad (#170-6515, #170-6516). The ImageJ software was used to perform densitometry analyses of western blots. Results for each band were normalized to the beta-actin/GAPDH levels in the same blot. The following antibodies for western blotting were purchased from cell signalling technology: PI3Kα (#4249), GSK3β S9 (#9322), GSK3β (#12456), β-catenin (#9582), TUBULIN (#2128). The following antibodies were purchased from Abcam: c-MYC (#32072), PI3K-p85α (#22653), UBE2C (#56861), UBE2T (#140611), lamin B1 (#16048). Beta-Actin (#A5316) and Vinculin (#V9131) were from SIGMA.

Nuclear-cytoplasmic fractionation

For the nuclear and cytoplasmic cell fractionation we used a centrifugation method. To obtain the cytoplasmic fraction, samples were lysed in ice-cold Nuclear Prep buffer (10 mM Tris-HCl pH 8.0, 100 mM NaCl, 2 mM MgCl2, 0,3M Sucrose, 0.2% NP40) plus protease inhibitors (Roche) and centrifugated at 3,000 rpm for 5 min. Subsequently, pellet containing nuclei were lysed in ice-cold S300 buffer (20 mM Tris-HCl (pH 8.0), 300 mM NaCl, 10% glycerol, 0.2% NP40) supplemented with protease inhibitors (Roche), sonicated and centrifugated at 13,000 rpm for 15 min to obtain nucleoplasmic fraction.

Cytokine and chemokine detection

To assess the effects of various treatments on cytokine and chemokine regulation cell lines were incubated with DMSO (0.1%), or different treatments for 24 hours and cell culture supernatants examined with a luminex multiplex assay (#HCYT-MAG-60K-PX41, Millipore), according to the manufacturer's instructions. Samples were run in duplicate and read using the luminex MAGPIX machine. Standard ELISA for MIP-1α was performed using the Quantikine MIP-1α human ELISA kit from R&D Systems, (#DMA00) according to manufacturer`s instructions.

Flow cytometry (Cell cycle analysis)

Cell Staining: Single cell suspensions were prepared and fixed with 70% fresh Ethanol for 2 hrs. After fixation, cells were washed twice with 1x PBS. Cells were then stained with neat (undiluted) Propidium Iodide (PI)/RNase Staining Solution (Cell Signaling, #4087) for 15 minutes at room temperature, protected from light before analysis. **Data Acquisition:** Flow cytometric data was acquired on a BD FACSCalibur (BD Biosciences, San Jose, CA) using CellQuest Pro Version 6.0. Propidium iodide was excited by the 488nm laser and fluorescence emission was measured in fluorescence parameter 3 (FL3) – with the standard 670LP filter. Greater than 10,000 events were acquired. **Data Analysis:** Doublets were excluded by gating out high FL3-W (width) cells.

Xenograft studies

6-week old NSG female mice were injected subcutaneously with 10 million TMD8 cells together with matrigel. Once tumors reached an average volume of 100 mm^3, mice were randomized to receive either vehicle control (5%DMSO/10% hydroxypropylbeta cyclodextrin) or CPI-203 at a dose of 5 mg/kg i.p. twice daily for 3 weeks. Combination experiments were performed in a similar manner: mice were randomized to receive either vehicle control, CPI-203 5 mg/kg i.p. twice daily, BKM-120 15 mg/Kg/daily by oral gavage, or both. Mice were observed daily throughout the treatment period for signs of morbidity/mortality. Tumors were measured three times weekly using calipers, and volume was calculated using the formula: length x $width^2 \times 0.52$. Body weight was also assessed three times weekly. After 3 weeks of treatment tumor samples were collected for immunoblotting.

Mass spectrometry studies data analysis

Lysis and in-situ digestion

The tryptic peptides were desalted by using stage tips (Thermo Scientific) using the manufacturer's instructions. The purified peptides were diluted to 0.1% formic acid, and each gel section was analyzed separately by microcapillary LC with tandem MS by using the NanoAcquity system (Waters) with a 100-inner diameter×10-cm lengthC18 column 1.7µm BEH130; Waters) configured with a 180-µm×2-cm trap column coupled to a Orbitrap Elite mass spectrometer (Thermo Fisher Scientific). Peptides were eluted with a 0-50% linear gradient of Acetonitrile

(0.1% formic acid) / Water (0.1% formic acid) over 200 mins at 300 nL/min. Key parameters for the mass spectrometer were: automatic gain control (AGC) 3×106 ions, resolution 120,000, m/z 300-1650 and a top 10 CID method.

MAXQUANT. All MS/MS samples were analyzed using MaxQuant (Max Planck Institute of Biochemistry, Martinsried, Germany; version 1.3.0.3) at default settings with a few modifications. The default was used for first search tolerance and main search tolerance: 20 ppm and 6ppm, respectively. Labels were set to Arg10 and Lys6. MaxQuant was set up to search the reference human proteome database downloaded from Uniprot on April 2, 2013. Maxquant performed the search assuming trypsin digestion with up to 2 missed cleavages. Peptide, Site and Protein FDR were all set to 1% with a minimum of 1 peptide needed for Identification but 2 peptides needed to calculate a protein level ratio. The following modifications were used as variable modifications for identifications and included for protein quantification: Oxidation of methionine, Acetylation of the protein N-terminus. Carbamidomethyl was used as a fixed modification for Cysteines. Raw data, Uniprot human fasta file as well as original MaxQuant result files can be provided upon request.

Scaffold. Maxquant results were imported into Scaffold Q+S (Proteomesoftware, Portland, Oregon, version 4.4.1). For Scaffold import, all default parameters were used against the same Uniprot human fasta file as searched in Maxquant. Scoring System was LFDR scoring with standard experiment wide protein grouping. Proteins and peptides were filtered at 1% FDR. For Q+S analysis, DMSO samples were organized as the reference channel. The JQ1 samples were organized as Category 1. Q+S normalization was done using the default protein reference.

Prime PCR IGF-1 signaling pathway array gene list

AKT1,AKT2,BAD,BCL2,BCL2L1,CASP9,CCND1,CCND2,CCND3,CDH1,CDKN1A,CHUK,COL1A1,CREB1,CRP,CTNNB1,EGFR,EIF4EBP1,ELK1,ERBB2,FOS,FOXO3,GAPDH,GRB2,GSK3A,

GSK3B,GYS1,HIF1A,HPRT1,HRAS,IGF1,IGF1R,IGF2,IGFBP1,IGFBP2,IGFBP3,IGFBP4,IGFBP5,IGFBP6,IKBKB,IL6,IRS1,IRS2,JUN,MAP2K1,MAP2K2,MAP3K5,MAPK1,MAPK3,MTOR,MYC,

NFKB1,NFKB2,NFKBIA,NFKBIB,NFKBIE,PDPK1,PIK3CA,PIK3CB,PIK3CD,PIK3R1,PIK3R2,

PIK3R3,PTEN,PTGS2,RAF1,REL,RELA,RELB,RHEB,RPS6KA1,RPS6KA2,RPS6KA3,RPS6KB1,
SERPINE1,SHC1,SOS2,SP1,SPP1,STAT3,TBP,TGFB1,TSC1,TSC2,UBA52,UBB,UBC,VEGFA,

YWHAB, YWHAE, YWHAZ

Ubiquitination pathway PCR array gene list

Ubiquitin-Activating Enzymes (E1)

ATG7, MOCS3, NAE1, NEDD8, SAE1, UBA1, UBA2, UBA3, UBA5.

Ubiquitin-Conjugating Enzymes (E2)

Regulation of Apoptosis: BARD1, BRCA1, TP53 (p53), UBE2Z.

Cell Cycle Regulators: ANAPC2, BARD1, BRCA1, CDC34, TP53 (p53), UBE2C, UBE2I.

Transcriptional Regulation: BRCA1, TP53 (p53), UBE2K, UBE2W.

Other Ubiquitin-Conjugating Enzymes (E2): ARIH1, BTRC (bTrCP), NEDD8, PARK2, STUB1, TMEM189, UBA6, UBE2A, UBE2B, UBE2D1, UBE2D2, UBE2D3, UBE2E1, UBE2E2, UBE2E3, UBE2G1, UBE2G2, UBE2H, UBE2J1, UBE2J2, UBE2L3, UBE2M, UBE2N, UBE2Q1, UBE2R2, UBE2S, UBE2T, UBR2.

Ubiquitin-Protein Ligases (E3)

Regulation of Apoptosis: BARD1, BRCA1, CUL1, CUL2, CUL3, CUL4A, CUL5, TP53 (p53), UBE4B, VHL.

Cell Cycle Regulators: ANAPC11, ANAPC2, BARD1, BRCA1, CUL1, CUL2, CUL3, CUL4A, CUL4B, CUL5, CUL7, DDB1, MDM2, CUL9, SKP1, SKP2, TP53 (p53), VHL.

Transcriptional Regulation: BRCA1, CBL, MDM2, SMURF2, TP53 (p53), VHL, WWP1.

Other Ubiquitin-Protein Ligases (E3): ARIH1, BRCC3, BTRC (bTrCP), DZIP3, FBXO3, FBXO31, FBXO4, FBXW10, FBXW9, HECW1, HECW2, HERC5, HUWE1, MARCH5, MIB1, MUL1, NEDD8, PARK2, RFWD2 (COP1), RNF123, RNF148, SMURF1, STUB1, SYVN1, UBE2L3, UBE2T, UBR1, UBR2.

References (supplemental methods)

Feller, W. (1971). An Introduction to Probability Theory and Its Applications. New York, USA. John Wiley&Sons.

R Core Team. R: A language and environment for statistical computing. (2014). R Foundation for Statistical Computing, Vienna, Austria. URL http://www.R-project.org/.

Tallarida RJ. (2001). Drug synergism: its detection and applications. J Pharmacol Exp Ther. *298*, 865-72.